MAGNETOHYDRODYNAMICS Vol. 44 (2008), No. 2, pp. 191–199

CONTRIBUTION OF HYSTERESIS LOSS TO THE HYPERTHERMAL EFFECT IN THE COBALT MAGNETIC FLUID

A. Skumiel[1], *A. Józefczak*[1], *A. Szlaferek*[2], *W. Kowalski*[2], *M. Timko*[3], *P. Kopčanský*[3], *M. Koneracká*[3]

[1] *Institute of Acoustics, Faculty of Physics, Adam Mickiewicz University, Umultowska 85, 61-614 Poznań, Poland*
[2] *Institute of Molecular Physics, PAS, Smoluchowskiego 17, 60-179 Poznań, Poland*
[3] *Institute of Experimental Physics, Slovak Academy of Sciences, Watsonova 47, Košice, Slovakia*

The paper reports results of hyperthermia experiments performed with a magnetic fluid containing $CoFe_2O_4$ particles subjected to a magnetic field of a few intensities ($0 < H_{AC} \leq 2350$ Am^{-1}) and at the frequency $f = 736$ kHz. To determine the structure of the fluid and its magnetic properties, the magnetic measurements were made by a vibrating sample magnetometer (VSM) in a field, whose intensity was changed in a wide range ($H = \pm 800$ kAm^{-1}). An additional study by the AFM method permitted estimation of the mean hydrodynamic volume of nanoparticles and the mean Brownian relaxation time of magnetisation. In the experimental conditions, the majority of the magnetic particles underwent demagnetization of the Brownian type [1]. In order to determine the percent contribution of the hysteresis loss P_h to the total energy loss P_{total}, a few hysteresis loops (VSM) have been determined for the magnetic field amplitudes typical of medical applications $H_{AC} < 30$ kAm^{-1}.

1. Introduction. Magnetic fluids are used in cancer treatment for hyperthermal destruction of tumours. Being magnetically soft granular materials of particle size close to 10 nm, they are superparamagnetics and usually do not show a hysteresis loop. The temperature of a magnetic fluid subjected to an external magnetic field increases rapidly because of the relaxation losses accompanying demagnetization. When a ferromagnetic particle is small enough and the ambient temperature is high enough, the energy of interactions between the particle's magnetic moment and its lattice can become small compared to k_BT. Thermal excitations can then redirect the magnetic moment away from the easy axis of the particle. The particle's single "super" moment is able to orient in any direction relative to the cluster lattice, with all directions being energetically nearly equivalent. The moment fluctuates under thermal agitation, and since all directions are equally probable, there is no zero-field magnetic moment. Superparamagnets, like all paramagnets, are soft magnetic objects, which retain no memory of previous magnetizations and have no area under their hysteresis curves. The phenomenon of superparamagnetism found in ferromagnetic clusters is completely analogous to classical Langevin paramagnetism. A superparamagnetic particle simply has one magnetic moment characterising the entire particle. This moment is essentially free to point in any direction relative to the particle lattice. When a magnetic field is applied, the moment tends to align with the field applied. However, what really changes is the Boltzmann distribution of possible orientations. In the presence of an external field the Boltzmann distribution is no longer isotropic and the time-averaged moment begins to point in the direction of the field applied. Only

at extremely high fields or very low temperatures the time-averaged magnetic moment will approach the full internal magnetic moment of the cluster.

The lowered energy is consistent with the principle that a more stable state is associated with the lower energy. When the fully magnetized material is removed from the field, the energy of the system increases because some work has been done on it to remove the material. The total energy is positive, and, since the only change from the original state of zero energy is the magnetization of the material, the energy of magnetization is positive. Its sign is easy to understand because energy has been absorbed during the process of magnetization by rotating the local magnetization against the forces of crystal anisotropy, by moving domain boundaries, and so forth.

2. Experimental details. The water-based magnetic fluid with $CoFe_2O_4$ particles was prepared by coprecipitation of aqueous solutions of $CoCl_2$–$FeCl_3$ mixtures in an alkali medium (in our case, NaOH).

A Vibrating Sample Magnetometer (VSM) measured the magnetic hysteresis loop of the magnetic fluid studied. The idea of VSM is based on the Faraday induction law and the original Foner solution [2]. Following Foner, the inventor of VSM, we used a loudspeaker for producing vibrations. The material under study in rgw VSM is inserted in a sample holder so that it rests centred in a pair of pickup coils between the poles of the electromagnet. A pair of stationary coils picks up the induced AC signal, which is proportional to the amplitude and frequency of the vibration and used as a control signal for modulation of the transducer. The output of the sample coil is fed to the differential input of a lock-in amplifier. The reference input of the lock-in comes from a sine wave oscillator used to drive the sample holder. The output of the lock-in goes to a data acquisition computer as well as the magnitude of the applied magnetic field coming from a gaussmeter.

The computer is now able to graph the magnetic moment of the sample against the applied magnetic field. When the sample is moved near a pickup coil, a voltage is induced in the coil. The voltage is proportional to the magnetic moment. The voltage induced in the detection coils is a function of many variables including the finite dimensions of the coils and sample, as well as the geometrical arrangement of the coil assembly vs. the sample. The VSM has traditionally been calibrated by

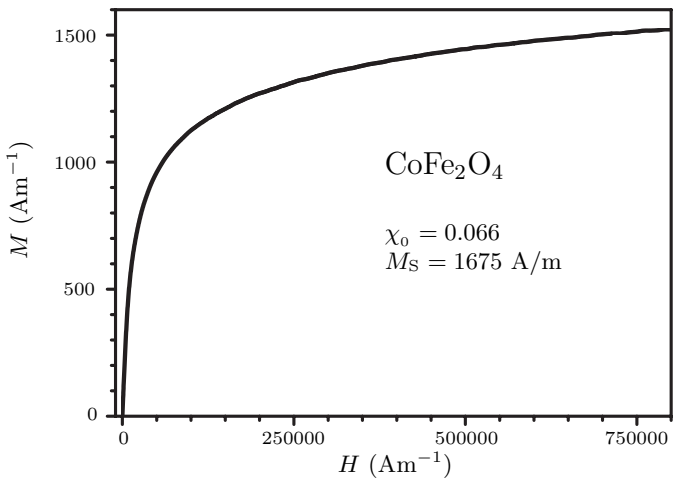

Fig. 1. The primary magnetization curve in a steady external magnetic field obtained from VSM measurements.

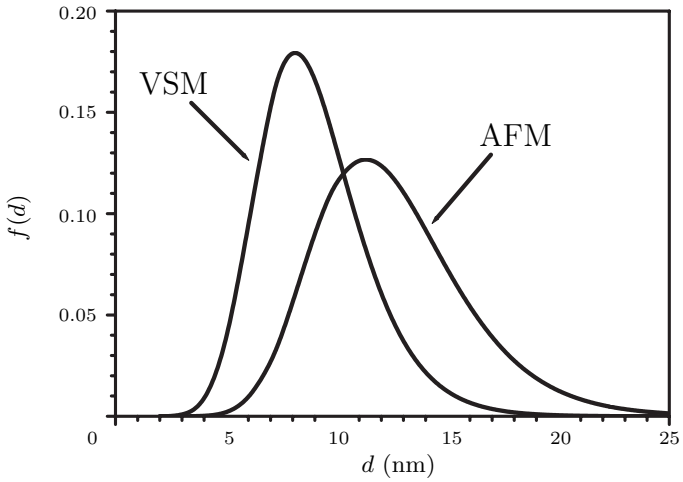

Fig. 2. Particle size distribution function obtained from VSM and AFM measurements.

using a small high purity nickel sphere as a standard [3]. The magnetic moment of the standard sample at saturation is known from the mass of the sphere and the voltage induced in the VSM coils is measured. This gives a calibration constant of VSM. Fig. 1 presents the magnetisation curve of a ferrofluid in the magnetic field changed within the range 0–800 $\mathrm{kAm^{-1}}$. On the basis of the measured results, the magnetisation of the sample in the saturated state has been estimated as $M_\mathrm{S} = 1675\,\mathrm{Am^{-1}}$. Then, knowing that $M_\mathrm{S} = M_\mathrm{g}\phi_\mathrm{V}$ (where $M_\mathrm{g} = 425\,\mathrm{kAm^{-1}}$), we could estimate the volume fraction of the solid phase as $\phi_\mathrm{V} \approx 0.39\%$. Taking into account the volume concentration of ferrite ϕ_V and its density ($\rho_\mathrm{ferrite} = 4.907\,\mathrm{g{\cdot}cm^{-3}}$), the authors calculated the mass of the magnetic material contained in a unit volume of the sample as $m_\mathrm{ferrite} = 0.0191\,[\mathrm{g_{ferrite}{\cdot}cm^{-3}_{sample}}]$.

The AFM method was applied to define the hydrodynamic size of nanoparticles. Fig. 2 shows the best fit of the lognormal functions for the distribution of magnetic diameters (VSM) and hydrodynamic diameters (AFM) from measurements of magnetic particles. The distribution function $f(d)$ is assumed to have the following lognormal form:

$$f(d) = \frac{1}{\sqrt{2\pi}d\beta} \cdot \exp\left[-\frac{\ln^2(d/d_0)}{2\beta^2}\right], \tag{1}$$

where d is the diameter, d_o and β are the parameters to be determined. Table 1 presents the mean diameters $\langle d\rangle$ and the mean standard deviations $\langle\sigma\rangle$ from $\langle d\rangle$ obtained by the VSM and AFM methods. The following formulae were used [4]:

$$\langle d\rangle = d_0 \cdot \exp\left(\frac{\beta^2}{2}\right)$$

and

$$\sigma = \langle d\rangle\sqrt{\exp^{\beta^2} - 1}. \tag{2}$$

The mean value of the nanoparticle volume was obtained from the distribution function $f(x)$ using the formula [1]:

$$\langle V\rangle = \frac{\pi}{6}\int_0^\infty d^3 f(d)\mathrm{d}d. \tag{3}$$

Table 1. The physical parameters of nanoparticles determined by the VSM and AFM methods.

method	d_0, nm	β	$\langle d\rangle$, nm	σ, nm	$\langle V\rangle$, nm^3	τ_N, s	τ_B, μs
VSM	8.7	0.263	9.0	2.4	466	6.9	-
AFM	12.1	0.265	12.5	3.4	1259	-	0.92

The mean relaxation time in the process of magnetization of the Néel and Brown types was found from the following equations [1]:

$$\langle\tau_N\rangle = \tau_0 \cdot \exp\left(\frac{K\langle V_m\rangle}{k_B T}\right)$$

and

$$\langle\tau_B\rangle = \frac{3\langle V_h\rangle}{k_B T} \cdot \eta, \tag{4}$$

where τ_0 ($\cong 1$ ns) is the time constant, $K = 200$ kJ·m^{-3} is the anisotropy constant for $CoFe_2O_4$, $k_B = 1.38 \cdot 10^{-23}$ J·K^{-1} is the Boltzmann constant, T is the absolute temperature, and $\eta \cong 10^{-3}$ N·s·m^2 is the viscosity of the carrier liquid. As implied by the data from Table 1, the Brownian mechanism of magnetisation is definitely dominant. A very high value of the effective anisotropy constant ($K = 200$ kJ·m^{-3}) for cobalt ferrite implies that under the conditions of our experiment the magnetisation of the nanoparticles occurs mainly due to the Brownian mechanism. According to the particle size distribution function obtained by the VSM, the largest grains of the diameters close to $d_m \cong 20$ nm (and, in particular, larger ones) can contribute to the loss of energy in hysteresis in the process of demagnetisation. Fig. 3 presents the courses of the relaxation times versus the magnetic radius of the particles due to the Néel and Brown mechanisms, assuming that the thickness of the surfactant layer (oleic acid) 2 nm corresponds to the length of the $C_{18}H_{36}O_2$ molecule. As follows from the plots, for the magnetic radius of $r_m \cong 3$ nm (equivalent to the hydrodynamic radius $r_h \cong 5$ nm) the two mechanisms bring the same contribution to the process of magnetisation.

Fig. 4 illustrates a few hysteresis loops $M(H)$ determined for the magnetic fluid studied in the range of the magnetic field recommended for the use in hyperthermia [5] (usually $H < 15$ kAm^{-1}). Table 2 presents the values of the parameters: remanence B_r, coercive field intensity H_C and the energy corresponding

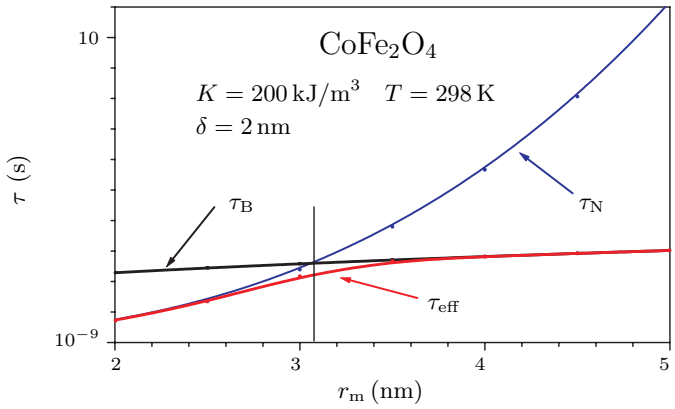

Fig. 3. Time constants vs. the particle size for $CoFe_2O_4$ nanoparticles.

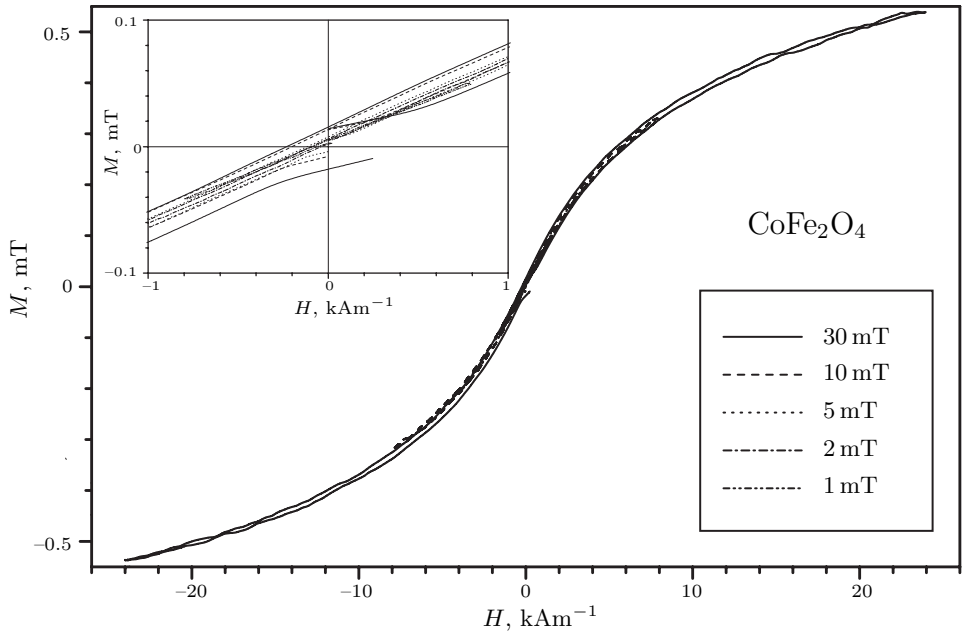

Fig. 4. Hysteresis loops $M(H)$ of a magnetic fluid with $CoFe_2O_4$ particles determined in a few ranges of the magnetic field used in hyperthermia.

to the area of the hysteresis loop, allowing estimation of the hysteresis loss in the total process of hyperthermic treatment. The measurements have shown that both the intensity of the coercive field H_C and the remanence B_r are not zero.

Technological details on the magnetic fluid hyperthermia experiments are given in [6].

3. Results and discussion. For magnetic fluids with superparamagnetic particles, the density of the thermal energy released in the magnetic fluid per unit of time is [7]:

$$P_r = f\Delta U = \mu_0 \pi \chi^{\parallel} f H^2, \tag{5}$$

where f is the frequency of alternating magnetic field in the sample, $\chi^{\parallel}$ is the imaginary magnetic susceptibility component. Under the adiabatic conditions, in such a medium, the rate of the temperature increase $\Delta T/\Delta t$ should be proportional to H^2. According to the experimental results of Hiergeist [8], for the fluids containing ferromagnetic particles of the size of a few tens of nm the rate of the

Table 2. Remanence B_r, coercive field intensity H_C and the magnetic hysteresis loss in the magnetic fluid studied for a few ranges of the magnetic field.

$\pm\Delta B$ [mT]	$\pm\Delta H$ [Am^{-1}]	B_r [μT]	H_C [Am^{-1}]	W_h [Jm^{-3}]	$P_h = f \cdot W_h$ [Wm^{-3}]	P_{total} [Wm^{-3}]	P_h/P_{total} [%]
1	796	0.9	10.6	0.0016	1178	16655	7.07
2	1592	1.8	27.3	0.0065	4784	77363	6.18
5	3979	3.9	59.1	0.044	32384	589132	5.5
10	7958	6.9	101.5	0.136	100096	$2.7{\cdot}10^6$	3.7
30	23873	12.2	185.8	0.41	301762	$31{\cdot}10^6$	1.0

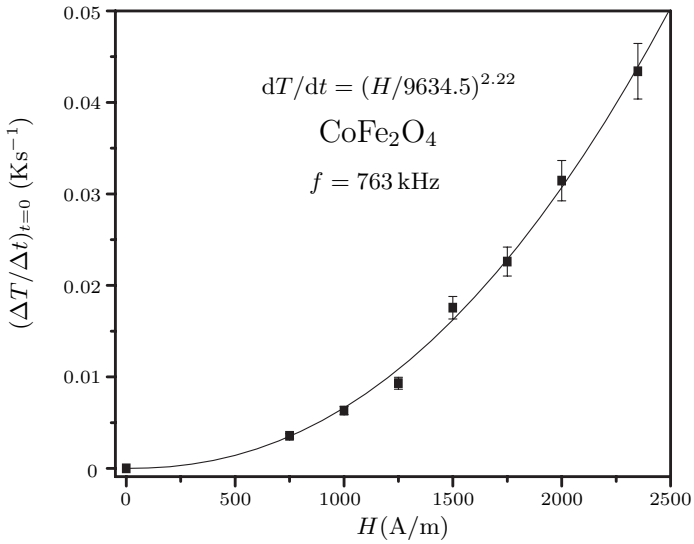

Fig. 5. The experimental values of $(\Delta T/\Delta t)_{t=0}$ as a function of the AC magnetic field amplitude (f = 763 kHz) and the plot of the fit with a function type $(H/a)^n$ for the magnetic fluid under study.

temperature growth $\Delta T/\Delta t$ is proportional to H^3. Assuming that as a result of polydispersion the magnetic fluid sample contains superparamagnetic (SPM) particles and those of greater size showing ferromagnetic properties (FM), the results of measurements have fit the following function:

$$\left(\frac{\Delta T}{\Delta t}\right)_{t=0} = \left(\frac{H}{a}\right)^n, \tag{6}$$

where a and n are the parameters of the fit. Fig. 5 presents the plot of the function and the results of measurements. The power n at H takes a value between 2 and 3 ($\cong$ 2.22). This value points to the presence of both superparamagnetic and ferromagnetic particles, which can be explained by their polydispersity. Therefore, there is another heat producing mechanism involved, following from the thermal energy loss for hysteresis. The amount of heat generated per unit volume is given by the frequency multiplied by the area of the hysteresis loop [5]:

$$P_{\mathrm{h}} = \mu_0 f \oint H \mathrm{d}M \quad [\mathrm{Wm}^{-3}]. \tag{7}$$

P_{h} was defined from quasi-static measurements of the hysteresis loop using a VSM magnetometer. In order to determine the percent contribution of the hysteresis loss P_{h} to the total energy loss P_{total}, a few hysteresis loops (VSM) were determined for the magnetic field amplitudes typical of medical applications $H_{\mathrm{AC}} < 30\,\mathrm{kAm}^{-1}$. Taking into account the two mechanisms of thermal energy production in a magnetic fluid, the total thermal energy released by a magnetic fluid can be described as [9]:

$$P_{\mathrm{total}} = P_r + P_{\mathrm{h}} = C_{\mathrm{s}} \cdot \rho_{\mathrm{s}} \cdot \frac{\Delta T}{\Delta t} \quad [\mathrm{Wm}^{-3}], \tag{8}$$

where C_{s} is the specific heat of the sample, ρ_{s} is the sample density. Fig. 6 presents the total density of heat power produced in the sample and the contribution of the hysteresis loop loss as a function of H^n. As follows from the calorimetric

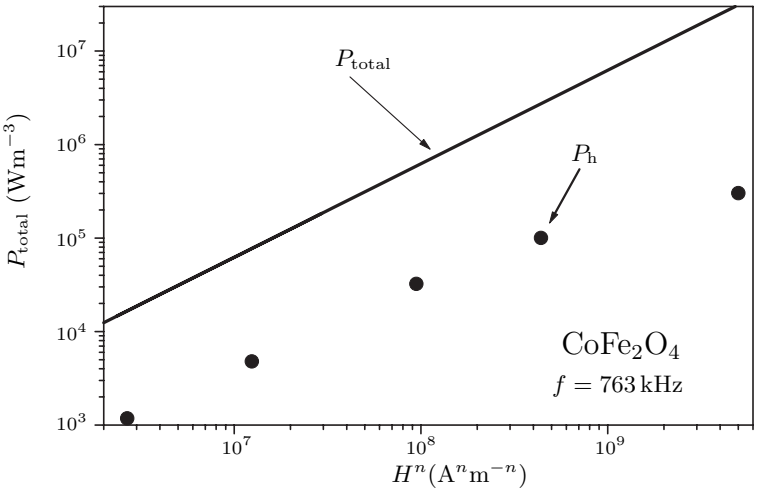

Fig. 6. Dependence of the total power (solid line) and hysteresis losses power (•) on H^n in the magnetic fluid with $CoFe_2O_4$ particles at $f = 763\,\text{kHz}$.

measurements and hysteresis loop measurements (VSM), the contribution of hysteresis to the total effect reaches only a few percent ($\leq 7\%$) and depends on the range of the magnetic field sweep $\pm\Delta H$. The higher the $\pm\Delta H$ values, the lower the contribution assigned to hysteresis. The dependence the coercive field H_{C} on the alternating magnetic field amplitude (Fig. 7) is nonlinear, and the higher the intensity of the demagnetizing field, the higher the value of H_{C}.

The specific absorption rate (SAR) values can be calculated from

$$\text{SAR} = \frac{C_{\text{s}}}{m_{sample}} \frac{\Delta T}{\Delta t}, \tag{9}$$

where C_{s} is the sample specific heat capacity, $(\Delta T/\Delta t)_{t=0}$ is the initial slope of the time-dependent temperature curve. The SAR [10] defined in the above way refers to the unit of the sample mass. Therefore, according to this definition, SAR is the heat released in 1 gram of the magnetic fluid. Taking into account that the specific heat of the carrier liquid is $C_{\text{H}_2\text{O}} = 4.18\ [\text{Jg}^{-1}\text{K}^{-1}]$ and the cobalt ferrite specific heat is $C_{\text{ferrite}} = 0.7\ [\text{Jg}^{-1}\text{K}^{-1}]$ and knowing their concentrations, the specific heat

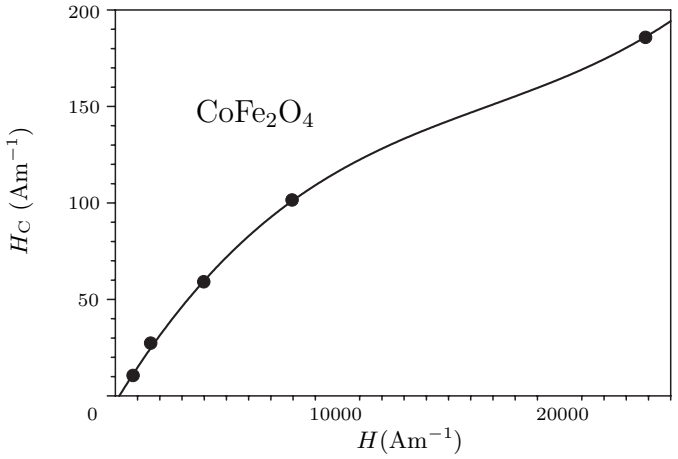

Fig. 7. The dependence of the coercive field H_{C} on the AC magnetic field amplitude.

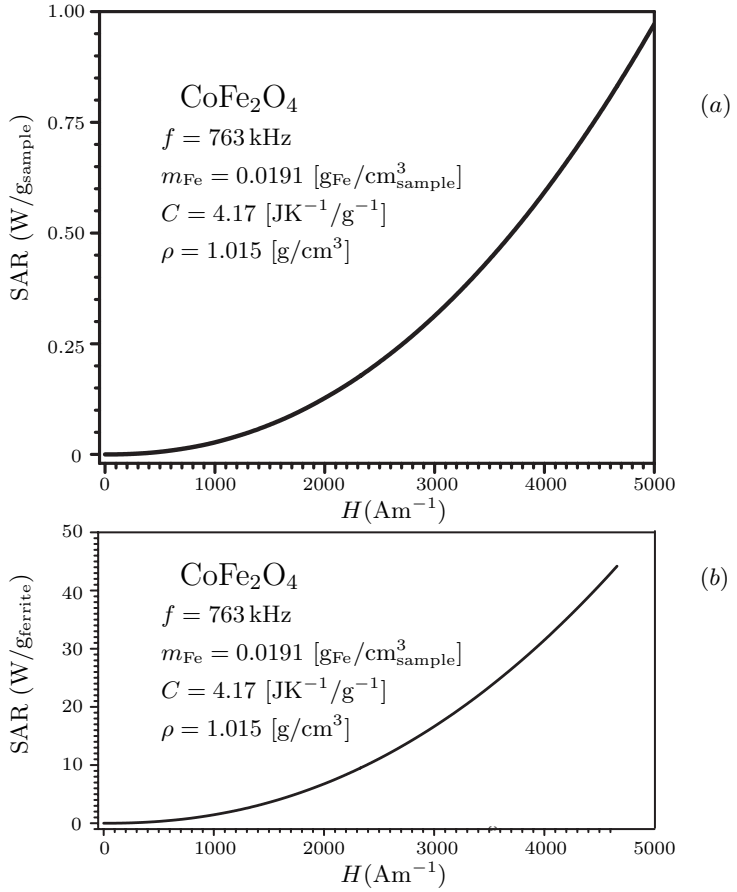

Fig. 8. The specific absorption rate functions referred to (*a*) the mass unit of the sample and (*b*) mass unit of the magnetic material in the magnetic fluid sample.

of the sample is estimated as $C_{\text{s}} = 4.169$ [Jg^{-1}K^{-1}]. Similarly, the density of the sample $\rho_{\text{s}} \cong 1.015$ [g·cm^{-3}] was calculated on the basis of the known densities and concentrations of the two components $\rho_{\text{H}_2\text{O}} \cong 0.997$ [g·cm^{-3}] and $\rho_{\text{ferrite}} \cong 4.907$ [g·cm^{-3}]. Fig. 8*a* shows the specific absorption rate dependence on the magnetic field intensity that can be expressed by the formula:

$$\text{SAR} = 4.169 \cdot \left(\frac{H}{9634.5}\right)^{2.22} [\text{W/g}_{\text{sample}}]. \tag{10}$$

The above equation derived from Eqs (6) and (9). The SAR value, ensuring the minimum intensity of the magnetic field required for therapeutic purposes $H_{\text{min}} = 2000\,\text{A/m}$, is thus $\text{SAR} = 0.13\,[\text{W/g}_{\text{sample}}]$.

A different definition of SAR referred to the mass unit of the magnetic material m_{ferrite} has been proposed in [11, 12]:

$$\text{SAR} = \frac{\rho_S C_S}{m_{\text{ferrite}}} \left(\frac{\text{d}T}{\text{d}t}\right)_{t=0} [\text{W/g}_{\text{ferrite}}]. \tag{11}$$

From the above formula, it is possible to evaluate and compare the suitability of different magnetic materials for their use in hyperthermia, irrespective of their

concentration in the magnetic fluid. Fig. 8*b* presents the course of SAR as referred to 1 gram of the cobalt ferrite mass. Assuming this definition, this function can be expressed numerically in the form:

$$\mathrm{SAR} = 221.54 \cdot \left(\frac{H}{9634.5}\right)^{2.22} \quad [\mathrm{W/g_{ferrite}}], \tag{12}$$

and its value for $H = 2$ kA·m^{-1} is 6.8 [W/g$_{\mathrm{ferrite}}$]. This value is 4 times greater than that obtained for the magnetic fluid with the magnetite grains of similar size, for which SAR $\cong 1.54\,[\mathrm{W/g_{ferrite}}]$ [13]. The sample of the magnetic fluid with the magnetite grains is magnetised mainly according to the Néel mechanism as the anisotropy coefficient for Fe_3O_4 is about 20 times lower ($K \cong 10$ kJ·m^{-3}).

4. Conclusion. The H^n denotes a law-type dependence of SAR, where $n = 2.22$ is the power at the amplitude of the magnetic field that testifies to the presence of superparamagnetic and ferromagnetic particles in the fluid sample. As follows from the calorimetric measurements and hysteresis loop measurements (VSM), the contribution of hysteresis to the total effect reaches only a few percent ($\leq 7\%$) and depends on the range of the magnetic field sweep $\pm\Delta H$.

Acknowledgements. This work was supported by the Slovak Grant Agency VEGA under contract No. 6166, the Technology Assistance Agency (APVV-99-026505 and APVT- 51-027904,) and the Polish Ministry of Science and Higher Education, Grant No. 4 T07B 04130.

REFERENCES

[1] B. Payet, D. Vincent, L. Delaunay, G. Noyel. *JMMM* **186** (1998), p. 168.

[2] S. Foner. *Rev. Sci. Instr.* **30** (1959), p. 548.

[3] J. Lindemuth, J. Krause. *IEEE Trans. Magn.* **37** (2001), p. 2752.

[4] M. Raşa. *Eur. Phys. J. E* **2** (2001), p. 265.

[5] Q..A. Pankhurst, J. Connolly, S.K. Jones, J. Dobson. *J. Phys. D: Appl. Phys.* **36** (2003).

[6] A. Skumiel. *JMMM* **307** (2006), p. 85.

[7] R.E. Rosensweig. *JMMM* **252** (2001), p. 370.

[8] R. Hiergeist, W. Andra, N. Buske, R. Hergt, I. Hilger, U. Richter, W. Kaiser. *JMMM* **201** (1999), p. 420.

[9] M. Ma, Y. Wu, J. Zhou, Y. Sun, Y. Zhang, N. Gu. *JMMM* **268** (2004), p. 33.

[10] S. Mornet *et al.* *Prog. Solid State Chem.* **34** (2006), p. 237.

[11] P. Pradhan P]*et al.* *J. Biom. Mater. Res. B: Appl. Biomaterials* 81B (2006), p. 12.

[12] J. Giri *et al.* *J. Appl. Phys.* **97** (2005), p. 10Q916.

[13] A. Skumiel, M. Labowski, H. Gojżewski. *Mol. Quant. Acoust* **28** (2007) (in press).

Received 02.04.2008